Infectious Disease Modelling 8 (2023) 617–631

Contents lists available at ScienceDirect

Infectious Disease Modelling

journal homepage: www.keaipublishing.com/idm

An exploration of the relationship between wastewater viral signals and COVID-19 hospitalizations in Ottawa, Canada

K. Ken Peng [a], Elizabeth M. Renouf [b, *], Charmaine B. Dean [b], X. Joan Hu [a], Robert Delatolla [c], Douglas G. Manuel [d, e, f]

[a] Department of Statistics and Actuarial Science, Simon Fraser University, 8888 University Dr, Burnaby, V5A 1S6, BC, Canada
[b] Department of Statistics and Actuarial Science, University of Waterloo, 200 University Ave W, Waterloo, N2L 3G1, ON, Canada
[c] Department of Civil Engineering, University of Ottawa, 75 Laurier Ave. E, Ottawa, K1N 6N5, ON, Canada
[d] The Ottawa Hospital Research Institute, 1053 Carling Ave, Ottawa, K1Y 4E9, ON, Canada
[e] Department of Family Medicine, University of Ottawa, 75 Laurier Ave. E, Ottawa, K1N 6N5, ON, Canada
[f] School of Epidemiology and Public Health, University of Ottawa, 75 Laurier Ave. E, Ottawa, K1N 6N5, ON, Canada

ARTICLE INFO

Article history:
Received 10 March 2023
Received in revised form 15 May 2023
Accepted 28 May 2023
Available online 7 June 2023
Handling Editor: Dr. Eftimie Raluca

Keywords:
Wastewater surveillance
COVID-19 vaccination effectiveness
Distributed lag nonlinear model
Time varying correlation

ABSTRACT

Monitoring of viral signal in wastewater is considered a useful tool for monitoring the burden of COVID-19, especially during times of limited availability in testing. Studies have shown that COVID-19 hospitalizations are highly correlated with wastewater viral signals and the increases in wastewater viral signals can provide an early warning for increasing hospital admissions. The association is likely nonlinear and time-varying. This project employs a distributed lag nonlinear model (DLNM) (Gasparrini et al., 2010) to study the nonlinear exposure-response delayed association of the COVID-19 hospitalizations and SARS-CoV-2 wastewater viral signals using relevant data from Ottawa, Canada. We consider up to a 15-day time lag from the average of SARS-CoV N1 and N2 gene concentrations to COVID-19 hospitalizations. The expected reduction in hospitalization is adjusted for vaccination efforts. A correlation analysis of the data verifies that COVID-19 hospitalizations are highly correlated with wastewater viral signals with a time-varying relationship. Our DLNM based analysis yields a reasonable estimate of COVID-19 hospitalizations and enhances our understanding of the association of COVID-19 hospitalizations with wastewater viral signals.

1. Introduction

Wastewater based epidemiology is currently an important tool for monitoring a wide range of behavioral, socioeconomic, and biological markers. Example of applications include regional/community drug abuse (Feng et al., 2018; Zuccato et al., 2005, 2008), industrial pollutant chemicals (Rousis et al., 2017), and polioviruses in the Global Polio Eradication Initiative (Asghar et al., 2014). During infection with the SARs-CoV-2 virus, SARS-CoV-2 ribonucleic acid (RNA) is excreted into the sewer system via feces, saliva, swabs and/or sputum of infected individuals (Anand et al., 2021; Peccia et al., 2020). This viral

* Corresponding author.
E-mail address: elizabeth.renouf@uwaterloo.ca (E.M. Renouf).
Peer review under responsibility of KeAi Communications Co., Ltd.

https://doi.org/10.1016/j.idm.2023.05.011

signal has been successfully detected in the city wastewater surveillance system using the RT-PCR technique (Medema et al., 2020; Randazzo et al., 2020). As testing of COVID-19 cases is limited, it is helpful to use wastewater surveillance data to track the prevalence of the COVID-19. Hegazy et al. (2022) and D'Aoust et al. (2021a,b) evaluated the time lagged correlation between wastewater viral signal and COVID-19 epidemiological data (laboratory positive cases, hospital admissions, ICU admissions, and deaths). Several studies investigated the possibility of using wastewater viral signals to predict COVID-19 epidemiological data (Galani et al., 2022; D'Aoust et al., 2021a).

A time lag was found to exist between the appearance of increased SARS-CoV-2 RNA signal in wastewater and epidemiological metrics (Larsen and Wigginton, 2020). D'Aoust et al. (2021a) showed that on average, there is an increase in SARS-CoV-2 viral RNA in wastewater 48 h before the increase is shown in COVID-19 clinical testing, and 96 h before an increase is seen in hospitalizations. Given the delayed association between COVID-19 indicators and wastewater viral signals, the use of the distributed lag model (DLM) is appropriate to explore the relationship between wastewater viral signal and COVID-19 epidemiology (Galani et al., 2022; Kaplan et al., 2021; Peccia et al., 2020; Schoen et al., 2022; Xie et al., 2022; Zulli et al., 2022).

DLMs have been widely used in social science (Judge, 1982) and epidemiology (Pope III and Schwartz, 1996). DLMs estimate the current value of the response variable based on the current value and the lagged values of explanatory variables, and the model has the following form:

$$E(Y_t|X_t, X_{t-1}, \ldots, X_{t-p}) = \alpha + \beta_0 X_t + \beta_1 X_{t-1} + \cdots + \beta_p X_{t-p}, \tag{1}$$

Gasparrini et al. (2010) extended this method to distributed lag nonlinear models (DLNM) which consider both nonlinear associations along the space of the predictor and in the lag dimension, simultaneously. This model has become popular in recent years and has been successfully applied to different fields. For instance, the lagged effect of air temperature on hospital admissions (Guo et al., 2021), the lagged association between climate variables and hospital admissions (Pedder et al., 2021), the lagged association between temperature and mortality (Entezari and Mayvaneh, 2019), and the association between long term exposures to PM2.5 and risk of acute respiratory infections among children and symptom onset (Larson et al., 2022). The nonlinear and time varying association between wastewater viral signals and COVID-19 hospitalizations is rarely discussed in current wastewater related literature. To fill this knowledge gap, we evaluated the nonlinear lagged association between wastewater viral signals and COVID-19 hospitalizations with a rolling correlation analysis, and then subsequently with a more sophisticated approach using the distributed lag nonlinear model. Since vaccination reduces the risk of hospitalization, we include vaccine efficacy as a covariate in our model, with a simulation of waning efficacy. Our approach enhances the understanding of the relationship between wastewater viral signals and COVID-19 hospitalizations and may inform decision making for allocation of health care resources, as stressors on health systems due to COVID-19 continue.

This paper is organized as follows. Section 2 describes the source of our wastewater surveillance data, hospitalization data, and vaccination information. Section 3 introduces an extension of the time step correlation analysis in Hegazy et al. (2022), and Section 4 introduces the distributed lag nonlinear model analysis with the consideration of simulated vaccination effectiveness against hospitalizations. In Section 5, we summarize the benefits of our project, and we also list the limitations of our model and some future research opportunities.

2. Data sources and descriptions

2.1. Wastewater surveillance data

We use data from Ottawa, Ontario, Canada, which is a city with a population of approximately 1 million inhabitants. Currently, wastewater samples at Ottawa are collected 7 days a week, analyzed and reported to public health and uploaded to github 5 days a week from the Robert O. Pickard Environmental Centre. This treatment facility serves 91.6% of Ottawa's population, and thus has good coverage for the related public health data provided by the Ottawa Public Health Unit. Pioneering research is being carried out at both the University of Ottawa and CHEO Research Institute on the methodology for measuring viral RNA in wastewater. The Ottawa data for viral copies of N1 and N2 genes are normalized using the biomarker pepper mild mottle virus (PMMoV). Detailed methodology addressing issues related to variation in wastewater surveillance are further described in D'Aoust et al. (2021a) and at https://613covid.ca/model/wastewater/. The wastewater data is available to download from the Canadian Open Wastewater Database, also called The Public Health Environmental Surveillance Database (PHESD), available at https://github.com/Big-Life-Lab/PHESD. During the 881 days in our study period, from June 16th, 2020, to November 13th, 2022, viral copies of N1 and N2 genes are measured on 744 days. The 60 missing dates occur mostly between June and September 2020, since daily collection was not started until September 2020. Arabzadeh et al. (2021) suggest that the spline method is a robust approach to cope with missing data in wastewater surveillance. Given that the sampling frequency and detection techniques of wastewater surveillance from different cities might be different, the imputation of the missing data in wastewater surveillance may need further investigation, e.g. with multiple sampling states, Dai et al. (2022) applied functional principle components analysis to impute missing values in wastewater surveillance data. For this project, 60 missing values of viral load were estimated by means of a smoothing spline regression. The average of normalized N1 and N2 gene concentrations was used to measure the wastewater viral signals, since they are both measuring the presence of SARS-CoV-2 in the wastewater.

2.2. COVID-19 hospitalization data

Data for COVID-19 hospitalizations are taken from the Open Ottawa dataset: COVID-19 Demographics and Source of Infection for Cases, Hospitalizations and Deaths, available at https://www.ottawapublichealth.ca/en/reports-research-and-statistics/daily-covid19-dashboard.aspx. From this dataset we used the variable, 'Cases_Currently_in_Hospital', the count of current hospitalizations as the response variable for our model in Section 4.2. This variable indicates the number of COVID-19 related patients who are still in hospital on a given day.

2.3. Vaccination information

Vaccination data for the Ottawa Public Health region is also considered in our analysis and is taken from the Ontario Data Catalogue, COVID-19 Vaccine Data by Public Health Unit, available here https://data.ontario.ca/dataset/covid-19-vaccine-data-in-ontario/resource/2a362139-b782-43b1-b3cb-078a2ef19524.

3. Correlation analysis

3.1. Motivation

During the 881 days of the study period (June 16, 2020, to November 13, 2022), the wastewater viral signal reached levels at or above 0.0001 copies/copies PMMoV on 681 days, 0.0002 copies/copies PMMoV on 524 days, 0.0005 copies/copies PMMoV on 252 days, 0.001 copies/copies PMMoV on 57 days, and 0.002 copies/copies PMMoV on only 8 days.

We observed that the trend of wastewater viral signal precedes the trend of COVID-19 hospitalizations, but there is much more variability in the wastewater viral signal, as day to day measurements fluctuate widely. We also observed that this association is not consistent over different waves (Fig. 1). For example, the count of COVID-19 hospitalizations aligns well with wastewater viral signals during the early waves through to the Alpha wave (June 2020, to June 2021), but the relationship is weak during the Delta wave (July 2021 to December 2021). Furthermore, during the Omicron BA.1 wave (December 2022 to February 2022), a relatively low level of wastewater viral signal was followed by a high level of COVID-19 hospitalizations, whereas during the Omicron BA.2 wave the opposite was observed. As noted in Hegazy et al. (2022), the reason for the lower hospitalizations during the BA.2 wave may be due to a combination of factors including the timing of the vaccination campaign for 3rd doses, and a high level of immunity from recent BA.1 infections.

Hegazy et al. (2022) performed a time step correlation analysis to evaluate the Spearman's rank correlation between the 5-day and 3-day midpoint average of wastewater viral signals and 5-days midpoint average of COVID-19 epidemiological data (laboratory positive cases, hospital admissions, ICU admissions, and deaths) with different lags, for each wave. In this section, we extend this time step correlation analysis by systematically calculating the Spearman's rank correlation between COVID-19 hospitalizations and the moving average of wastewater viral signals by allowing different time windows for the moving average of wastewater viral signals, different lag days, and breaking the study period into different time frames based on the availability of vaccines and the arrival of the more transmissible Omicron variant.

3.2. Method

The approach described below investigates the following questions: 1) What is the optimized choice of τ_1 and τ_2 in terms of the correlation between wastewater viral signal and COVID-19 hospitalization in each of the three periods? 2) How does the optimized correlation $argmax_{\tau_1,\tau_2}(R(\tau_1,\tau_2))$ between wastewater viral signal and COVID-19 hospitalization vary over time? 3) How do the values of τ_1 and τ_2 vary over time? We used the idea of rolling correlation with 100 days as the rolling window and calculate Spearman's correlation between wastewater viral signals and COVID-19 hospitalizations. By using Spearman's correlation, we are able to identify the monotonic association between these variables rather than the linear

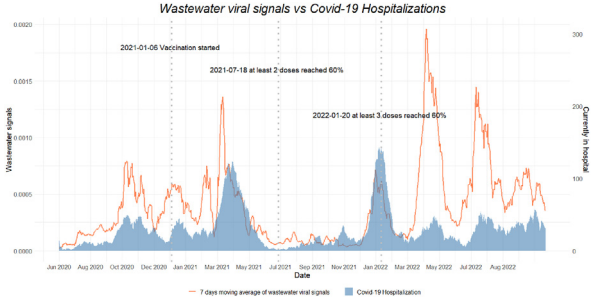

Fig. 1. 7-day moving average of N1–N2 average viral signal and COVID-19 hospitalizations counts.

association. Let τ_1 be the time-lag between wastewater viral signals and COVID-19 hospitalizations; τ_2 be the time window of the moving average (MA) of the wastewater viral signals; W_t be the wastewater viral signals on day t, $t = 1, 2, \ldots, 100$ for each rolling window; Y_t be the number of COVID-19 hospitalizations on day t. For each rolling window, we perform the following algorithm.

Algorithm 1.

Algorithm 1

1: Calculate $MA_{\tau_2}(W)_t$.
2: Calculate $R(\tau_1, \tau_2)$

$$R(\tau_1, \tau_2) = \frac{\sum_{i=1}^{100}(rk(MA_{\tau_2}(W)_i) - 50.5)(Y_{i+\tau_1} - \overline{Y})}{\sqrt{\sum_{i=1}^{100}(rk(MA_{\tau_2}(W)_i) - 50.5)^2}\sqrt{\sum_{i=1}^{100}(Y_{i+\tau_1} - \overline{Y})^2}}, \quad (2)$$

3: Repeat 1, 2 with τ_1 and τ_2 from 1 to 20.
4: Choose the values of τ_1 and τ_2 where $(\tau_1, \tau_2) = argmax_{(\tau_1,\tau_2)}R(\tau_1, \tau_2)$

Here $MA_{\tau_2}(W)_t$ is the moving average of the wastewater viral signal on day t over τ_2 days. $R(\tau_1)$ is the cross correlation between COVID-19 hospitalizations and τ_2 days moving average of wastewater viral signals using Spearman's method. $rk(MA_{\tau_2}(W)_i)$ is the rank of the $MA_{\tau_2}(W)_i$ within the given rolling window, this rank is from 1 to 100 and the average $rk(MA_{\tau_2}(W)_i) = 50.5$.

Note that to calculate the moving average of the wastewater viral signal on day i, we use only historical data from day i, $i - 1, \ldots, i - \tau_2$ and the optimized correlations are obtained when the hospitalizations on day i, Y_i aligns with $(W_{i-\tau_1} + W_{i-(\tau_1+1)} + , \ldots, W_{i-(\tau_1+\tau_2)})/\tau_2$.

3.3. Results

Table 1 shows the results of the correlation analysis for 3 selected rolling windows as an example. The columns titled optimized τ_1 and the optimized τ_2 show the value of τ_1 and τ_2 which maximize the Spearman's correlation between the moving average of the wastewater viral signals and COVID-19 hospitalizations in the corresponding period. For example, the first row shows that during the period June 16th, 2020, to September 23rd, 2020, a 17-day moving average of the wastewater viral signal with 1 day lagged between wastewater signal and hospitalizations had the highest optimal correlation.

The value of $\tau_1 + \tau_2$ represents the furthest time lag used to construct the optimized correlation with wastewater viral signals and COVID-19 hospitalizations. We observed that the optimized $\tau_1 + \tau_2$ and the optimized correlation vary across time (Fig. 2).

Recall that the optimized correlations are obtained when the hospitalizations on day i, Y_i are aligned with $(W_{i-\tau_1} + W_{i-(\tau_1+1)} + , \ldots, W_{i-(\tau_1+\tau_2)})/\tau_2$. The value of the optimized $\tau_1 + \tau_2$ shown in Fig. 2 has a rapidly oscillating structure. By manually checking those dates, we found that the value of the optimized $\tau_1 + \tau_2$ increases while COVID-19 hospitalizations are on the way up, and decreases while COVID-19 hospitalizations are on the way down. Around Aug 2020, Nov 2021, Dec 2021, and mid-Feb 2022, the value of the optimized $\tau_1 + \tau_2$ have small values which suggest that individuals are admitted to hospital quickly during those periods. Interestingly, during the second half of the Delta period, the values of the optimized $\tau_1 + \tau_2$ are large, which may indicate that individuals are admitted to hospital more slowly. We also show the optimized τ_1 and τ_2 in the third plot in Fig. 2. We observed that the curve of optimized τ_1 is flatter than the curve of optimized τ_2 over time. τ_1 is the time lag between hospitalizations and the smoothed wastewater viral signals, which varied between 1 and 10 days, for the most part, but was as large as 15 days during the Delta wave. τ_2 is the time window used to smooth out the wastewater viral signal, and it rapidly oscillates when the daily wastewater viral signals change fast. The correlation between wastewater viral signal and COVID-19 hospitalizations is overall very high, and this confirms the monotonic association between wastewater viral signals and COVID-19 hospitalizations. The increases in wastewater viral signals reflect the increases in COVID-19 hospitalizations in the future. However, there was a noticeable large drop for the optimized correlation. During the periods from July 2021 to Oct 2021, COVID-19 hospitalizations are weakly correlated with wastewater viral signals. This finding is similar to the results in Hegazy et al. (2022).

Table 1
Example of optimization of τ_1 and τ_2 from the rolling correlation process.

Period	Optimized τ_1	Optimized τ_2	Optimized $R(\tau_1, \tau_2)$
2020-Jun-16 to Sep-23	1	17	.773
…	…	…	…
2020-Aug-01 to Nov-09	5	11	.852
…	…	…	…
2021-Aug-09 to Nov-11	18	3	0.126

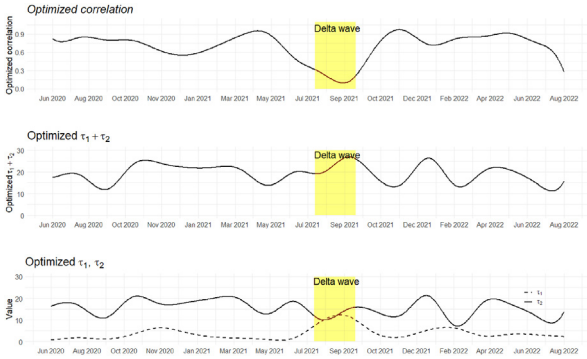

Fig. 2. The optimized correlation over time (upper plot), the optimized τ_1 + optimized τ_2 over time (middle plot), and optimized τ_1, τ_2 over time. Smoothed using cubic smoothing spline.

4. Nonlinear model with random lag

4.1. Vaccination information

A major influence on the time varying correlation between wastewater signals and hospitalizations is popular immunity from vaccination or infection. The time varying correlation observed might be caused by changing levels of population immunity after COVID-19 vaccination campaigns. The COVID-19 vaccine was first available in Jan 2021 in Ottawa. The percentage of the fully vaccinated (at least two doses) population reached 60% on July 18th, 2021, and the percentage of those boosted over age four (at least 3 doses) reached 60% at Jan 20th, 2022. We consider the vaccine effectiveness (VE) as a numeric variable measuring how well vaccination protects people against hospitalization at the population level.

It is important to investigate whether waning vaccine effectiveness might influence our model examining the relationship between wastewater viral signal and hospitalizations. However, without having detailed individual level vaccination information, we consider a simplified approach. Specifically, for each dose of the vaccine, we simulated the VE curve across our study period (June 16th, 2020, to November 13th, 2022) based on assumptions of effectiveness as described in the three scenarios below.

Let v_{ijs} be the VE of the *jth* vaccine received on day i, to day s, where the i and s take values from 1 to 881. The value of VE is between 0 and 1 and $v_{ijs} = 0$ when $s < i$, $v_{ijs} \in (0, 1]$ when $s \geq i$, for instance, the vaccine received on day 10 will not count towards effectiveness on day 1. By adding up all $v_{\cdot\cdot s}$, we obtain V_s^*, the simulated number of cumulative vaccine doses which are still effective against hospitalizations on day s

$$\sum_{i=1}^{881} \sum_{j=1}^{N_i} V_{ijs} = V_s^*, \tag{3}$$

where N_i represents the number of vaccine doses received on day i.

4.1.1. Scenario 1

We first make a strong assumption that each dose of the vaccine will contribute to reduction of COVID-19 hospitalizations immediately and will not wane over time. Under this scenario, $v_{ijs} = 1$ for all $s \geq i$, $V_s^* = V_s$ for all $s = 1, \ldots, 881$.

4.1.2. Scenario 2

We weaken our assumption to assume that the *jth* vaccine received on day i will contribute to reduction of COVID-19 hospitalizations after T days, and the vaccine effectiveness against hospitalization starts at 100% and decreases θ percentage per day where T and θ are random for each dose of the vaccine. Under these assumptions:

$$v_{ijs} = \begin{cases} 0 & s - i < T_{ij}, \\ 1 & s - i = T_{ij}, \\ v_{ij(s+1)} - \theta_{ij}(s - (i + T_{ij})) & s - i > T_{ij}. \end{cases}$$

Ssentongo et al.'s meta-analysis (Ssentongo et al., 2022) found eleven studies reporting vaccination effectiveness starting within 7 days of the second dose of the mRNA vaccine, and two studies reporting VE starting after 14 days of the second dose of mRNA vaccines. They also conclude that protection of vaccination against severe COVID-19 remained high through 175 days after vaccination, and the estimated VE was 90% (89–92%) at 5 months following vaccination. In order to allow for individual variability, we further assume that T and θ are both random and follow a normal distribution $T \sim N(14, 3^2)$, and $\theta \sim N(0.1\%, 0.01\%^2)$ for all i, j. By applying this scenario, the VE of a single dose will be centered around 82% after 194 days.

4.1.3. Scenario 3

A drawback of scenario 2 is that Ssentongo's meta-analysis (Ssentongo et al., 2022) was conducted before the emergence of the Omicron variant. The VE against severe disease after two doses has been found to be lower against the Omicron variant (Andrews et al., 2022; Thompson, 2022). Ferdinands et al. (2022, p. 379) evaluated the VE against COVID-19 hospitalizations during the Omicron period by different age groups, vaccine product, and immunocompromised status. Therefore, we simulate scenario 3 based on the adjusted VE in Table 2 in Ferdinands et al. (2022, p. 379).

First, we keep the assumption that each dose of the vaccine will contribute to the reduction of COVID-19 hospitalizations after T days. In addition, we consider that dose 1, dose 2, dose 3, and dose 4 are different and we add a superscript to represent dose 1–4, e.g. $v_{ijs}^{(k)}$ represents the VE of the dose k. The values of $v_{ijs}^{(k)}$ are shown in Table 2.

The V_s^* under different scenarios are shown in Fig. 3. The initial drop at the start of scenario 3 represents the drop in VE against severe disease with the arrival of the Omicron variant. We noticed that depending on our assumptions of scenario 3, the cumulative VE is currently decreasing, because vaccine uptake by the population of Ottawa has declined. The average number of daily doses received by the Ottawa population was over 3000 through the pre-Omicron period, and it declined to less than 2000 in the last two month of the study period.

4.2. Distributed lag nonlinear model

Given the complexity of the nonlinear association between wastewater viral signal and COVID-19 hospitalizations, we employed a Poisson additive model under the framework of the DLNM. The DLNM is a flexible model and allows effects that vary simultaneously both along the space of the predictor and in the lag dimension of its occurrence (Gasparrini et al., 2010). The model uses cross-basis functions to transform the original explanatory variable to a set of basis variables, and then the basis variables can be fitted into other models as a regular set of variables. The cross-basis functions consist of two sets of basis functions. We used polynomial smooth functions with degree 2 to describe the associations between wastewater viral signals and COVID-19 hospitalizations along the space of the predictor (wastewater viral signal) and in the lag dimension. We assume that the time lag between infected individuals producing wastewater viral signals and the individuals being admitted to the hospital is a random variable varying from 0 to 15 days. Therefore, we consider a lag range between 0 and 15 days in our population level model. The intercept of the model is constructed as a function of time t with smooth functions. By testing different smooth functions, we decided to use P-splines (Penalized splines) which produced the smallest Akaike information criterion (AIC). P-splines were first proposed by Eilers and Marx (Eilers and Marx, 1996). We use a time varying intercept to capture the monthly contributions of other factors not included in the model such as public health interventions, or properties of different variants of concern. Ideally, the effect of the intercept should not be strong, otherwise, this may indicate the model is missing some important variables. In addition, the adjusted vaccination contribution to the COVID-19 hospitalizations described in Section 3.4.1 is included in the model. Let Y_t be the number of COVID-19 cases in hospital on day t; V_t^*, the simulated number of cumulative vaccine doses which are still effective against hospitalizations on day t described in Section 3.4.1. Our model can be written as:

$$\log(E(Y_t|W_t, V_t^*)) = \alpha + f(t) + S(W_t;\beta) + \gamma V_t^*, \tag{4}$$

Table 2
Simulation of $v_{ijs}^{(k)}$ based on Table 2 in Ferdinands et al. (2022).

Dose	Vaccine effectiveness	Condition
Dose 1: $v_{ijs}^{(1)}$	0	$s-i<T_{ij}^{(1)}$
	$N(.58, .02^2)$	$s-i\geq T_{ij}^{(1)}$
Dose 2: $v_{ijs}^{(2)}$	0	$s-i<T_{ij}^{(2)}$
	$N(.73, .02^2)$	$60>s-i\geq T_{ij}^{(2)}$
	$N(.61, .02^2)$	$120>s-i\geq 60$
	$N(.57, .02^2)$	$180>s-i\geq 120$
	$N(.48, .02^2)$	$240>s-i\geq 180$
	$N(.51, .02^2)$	$300>s-i\geq 240$
	$N(.55, .02^2)$	$360>s-i\geq 300$
	$N(.40, .02^2)$	$420>s-i\geq 360$
Dose 3: $v_{ijs}^{(3)}$	0	$s-i<T_{ij}^{(3)}$
	$N(89, 2^2)$	$60>s-i\geq T_{ij}^{(3)}$
	$N(.86, .02^2)$	$120>s-i\geq 60$
	$N(.66, .02^2)$	$180>s-i\geq 120$
	$N(.41, .02^2)$	$240>s-i\geq 180$
	$N(.31, .02^2)$	$300>s-i\geq 240$
	$N(.32, .02^2)$	$s-i\geq 300$
Dose 4: $v_{ijs}^{(4)}$	0	$s-j<T_{ij}^{(4)}$
	$N(.75, .02^2)$	$60>s-j\geq T_{ij}^{(4)}$
	$N(.54, .02^2)$	$s-i\geq 60$

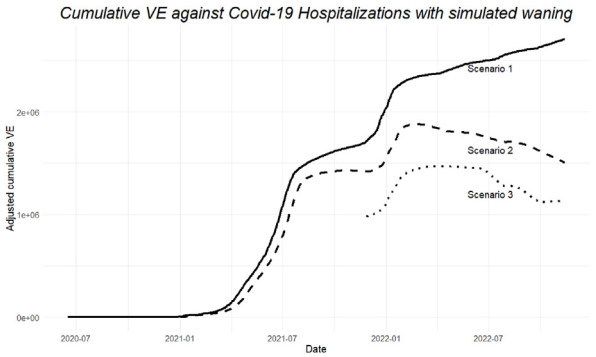

Fig. 3. The simulated vaccine effectiveness (VE) against COVID-19 hospitalizations under different waning assumptions. The x-axis represents the date of vaccination for any dose with the y-axis being the value of V_s^* defined in equation (3).

Here γ is an unknown parameter describing the linear association between V_t^* and $\log(Y_t)$; α is a fixed intercept, and $f(t)$ is a smooth function of time t, compressed to vary monthly, $\alpha + f(t)$ can be considered as the time varying intercept which summarizes the monthly contribution of other factors, e.g. population immunity from seroprevalence, government interventions. This time varying intercept serves to control the information that are not explained by the wastewater viral signals and VE; W_t is a vector of historical wastewater viral signals at time t, e.g., wastewater viral signals on day $t, t-1, \ldots, t-15$; the term $S(W_t; \beta)$ represents the transformed wastewater viral signals with the selected cross-basis functions, and the vector β contains the corresponding unknown parameters that need to be estimated. The association between wastewater viral signals and COVID-19 hospitalizations is represented as relative risk (RR), which measures the ratio of the risk for COVID-19 hospitalizations for the exposure group to the risks for the non-exposure group. Specifically, RR equal to 1 indicates that there is no association between wastewater viral signals and COVID-19 hospitalizations; RR > 1 indicates a positive association between wastewater viral signals and COVID-19 hospitalizations; RR < 1 indicates the negative association between wastewater viral signals and COVID-19 hospitalizations. Various data visualizations are provided to summarize the association between wastewater viral signal and COVID-19 hospitalizations. For comparison, we also fitted the distributed lag model (DLM)

$$\log(E(Y_t|W_t, V_t^*)) = \alpha + f(t) + \sum_{d=1}^{D} \beta_d W_d + \gamma V_t^*, \tag{5}$$

The DLM considers the linear association between the wastewater viral signals and hospitalizations, the $\sum_{d=1}^{D} \beta_d W_d, d = 1, \ldots, D$ is a linear combination of historical wastewater viral signals.

The arrival of the Omicron variant in November 2021, brought with it a more transmissible virus at a time when population immunity was boosted by recent vaccination campaigns in Ottawa. Therefore, our model (4) was applied to the pre-Omicron and Omicron periods separately to investigate how the association between the wastewater viral signal and COVID-19 hospitalization during the Omicron period (Nov 27th, 2021 to Nov 13th, 2022) changes compared to the pre-Omicron period (Jun 16th, 2020 to Nov 26th, 2021). The analysis was carried out using R software (version 4.1.1) with packages dlnm (version 2.4.7, Gasparrini, 2011) and mgcv (version 1.8–36, Wood, 2017).

4.3. Lag associations between wastewater viral signal and COVID-19 hospitalizations

We observed that the distributed lag nonlinear model using wastewater viral signal as a surrogate for exposure can capture the true trend of COVID-19 hospitalizations with the adjusted $R^2 > 0.90$ for the pre-Omicron period and $R^2 > 0.94$ for the Omicron period. The AIC values from the DLM (Table 4) are higher than the AIC values from the DLNM for all three scenarios. The estimated γ is negative for both the pre-Omicron period and the Omicron period in the DLNM (Table 3) under all scenarios, while the p-values were significant for both the pre-Omicron period and the Omicron period. This shows that in

Table 3
Adjusted R^2 and estimated γ of the model under different scenarios using DLNM. The p-value < 0.05 rejects the null hypothesis H_0: $\gamma = 0$.

Scenario	Period	**Adjusted R^2**	AIC	$\hat{\gamma}$ (p-value)
Scenario 1	Pre-Omicron	.904	3623.4	-1.7×10^{-6}(.00)
	Omicron	.944	2221.7	-6.0×10^{-7}(.02)
Scenario 2	Pre-Omicron	.905	3637.7	-2.0×10^{-6}(.00)
	Omicron	.946	2223.9	-6.2×10^{-7}(.00)
Scenario 3	Omicron	.946	2221	-4.9×10^{-7}(.03)

Table 4
Adjusted R^2 and estimated γ of the model under different scenarios using DLM. The p-value < 0.05 rejects the null hypothesis H_0: $\gamma = 0$.

Scenario	Period	**Adjusted R^2**	AIC	$\hat{\gamma}$ (p-value)
Scenario 1	Pre-Omicron	.828	4126.8	-1.8×10^{-6}(.00)
	Omicron	.917	2345	1.1×10^{6}(.00)
Scenario 2	Pre-Omicron	.821	4171.6	-1.8×10^{-6}(.00)
	Omicron	.915	2368	-1.1×10^{-7}(.57)
Scenario 3	Omicron	.914	2367	-2.3×10^{-7}(.25)

our model, the number of vaccine doses contribute to a reduction in hospitalizations due to COVID-19. However, in our model, a higher effect of population level vaccination is seen in the pre-Omicron period during which time the number of doses increased the most. During the Omicron period, the change in the number of doses is comparatively flat. Our data does not include individual level data on vaccination status of the hospitalized individuals. We can speculate that reasons for a somewhat reduced effect in the model for the Omicron period are likely related to a combination of factors, including that the number of doses changes very little during the Omicron period compared to the previous period when vaccination began. Two time series plots of estimated COVID-19 hospitalizations and observed COVID-19 hospitalizations under scenario 3 are provided in Fig. 4. Note that scenario 3 and scenario 2 have the same assumption for the pre-Omicron period.

To investigate how hospitalizations would change if the vaccination rate was different, we provide estimates for hospitalizations under two scenarios where doses are reduced by 10% and by 50%. To do this, we repeated the simulation in Section 4.1.3 under scenario 3 to obtain the V_t^* in model (4). Fig. 5 shows the model predicted hospitalizations if vaccine doses are reduced by 10% or 50%, while the wastewater level is unchanged. Under our simulation, COVID-19 hospitalizations would increase dramatically the delta wave if vaccine uptake was reduced. During the Omicron period, the simulated reduction in vaccine uptake results in an increase in hospitalizations, especially in January 2022, and then less so in the weeks following. Recall that the changes in the number of doses in the Omicron period are relatively flat compared to the pre-Omicron period, and the calculations for this simulation are based on maintaining the wastewater signals at the same level.

Fig. 6 shows the relative risk (RR) of COVID-19 hospitalizations over different levels of wastewater viral signals at time lag = 0, lag = 5, lag = 10, and time lag = 15 for both the pre-Omicron period and the Omicron period. The upper/lower bound of the 95% confidence interval is also plotted. The interpretation of the results is straightforward, e.g., during the pre-Omicron period, if the wastewater viral signal is at level 0.0002 copies/copies PMMov on day $(t - 15)$, then the expected COVID-19 hospitalizations on day t is about 1.05 (1.04–1.06) times higher than the baseline (wastewater viral signal = 0) expected COVID-19 hospitalizations on day t.

We observed that the RR of COVID-19 hospitalizations increases when wastewater viral signals are high, no matter the value of the time lag. This illustrates that the wastewater viral signal can be used as a predictive marker signalling future increases in COVID-19 hospitalizations. Another important observation is that the association between wastewater viral signal and COVID-19 hospitalizations is not significant at a small time lag (lag = 0) or at a large time lag (lag = 15) during the Omicron period (see Fig. 6, column 1 row 3 plot, and column 2, row 4 plot). Similarly, Fig. 6 shows the RR of COVID-19 hospitalizations over different lags at different wastewater viral signal levels (median, 95% percentile) for both the pre-Omicron period and Omicron period. We observed that the association between wastewater viral signals and COVID-19 hospitalizations is different during the pre-Omicron period and the Omicron period. During the pre-Omicron period, the RR is at the highest level when the lag is small, and it increases slightly when the time lag gets larger, beginning around lag of 10 days (Fig. 6). During the Omicron period, the RR is not significant at small time lags (i.e., < 1), but it increases to the highest risk around a lag of 9 days, then decreases again. This may be explained by the timing of the vaccination campaign and the

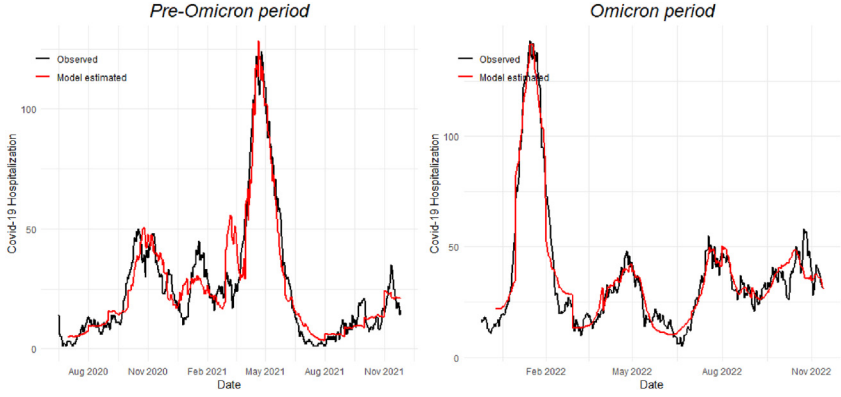

Fig. 4. Model predicted COVID-19 hospitalizations and observed COVID-19 hospitalizations over time for pre-Omicron and Omicron periods. The model shown is under scenario 3 of the vaccine effectiveness simulation.

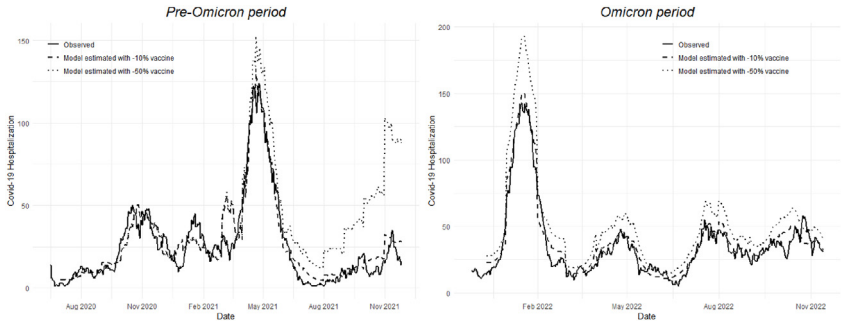

Fig. 5. Observed, and model predicted COVID-19 hospitalizations if the vaccine doses are reduced by 10% or 50%. The model shown is under scenario 3 of the vaccine effectiveness simulation.

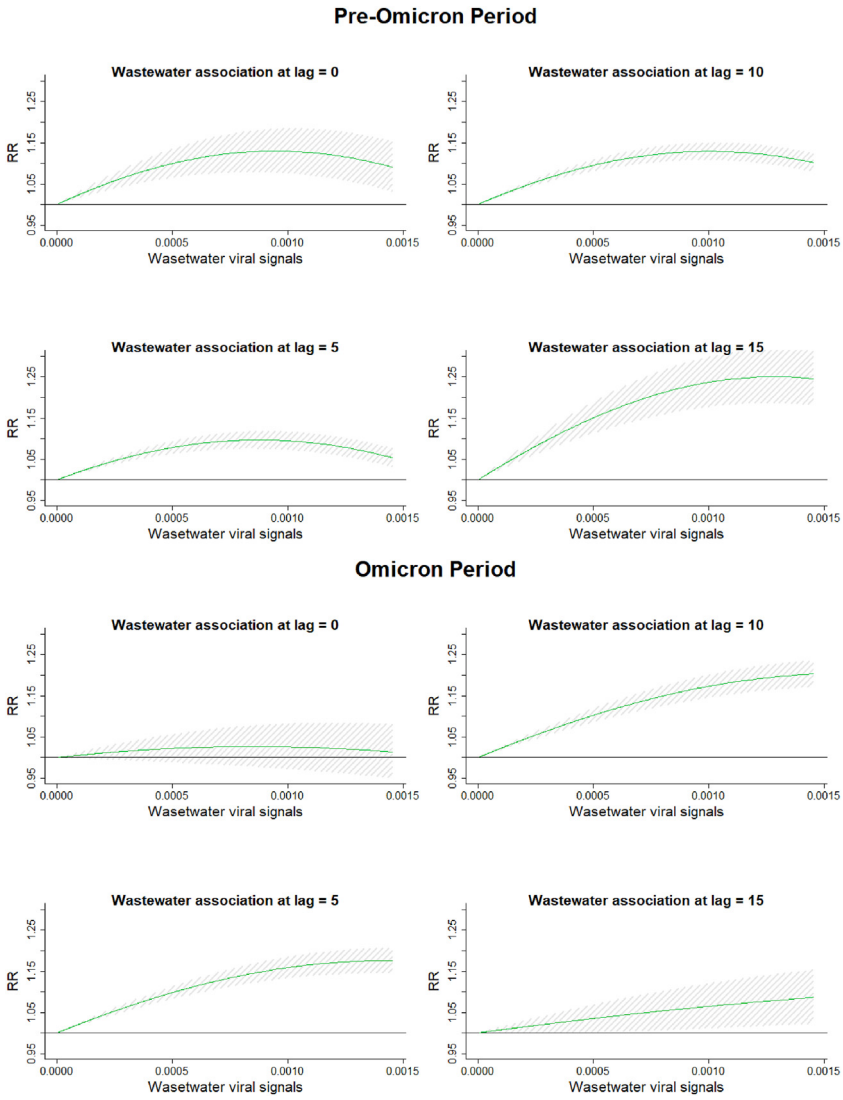

Fig. 6. Relative risk of COVID-19 hospitalizations at specific time-lag for pre-Omicron and Omicron period.

third dose campaign. We saw our highest levels of wastewater signal during the Omicron BA.2 wave when 93% of the population had protection from two doses, and a third dose campaign was underway. Thus, while there was a great deal of virus present in the wastewater, protection from severe disease via vaccination kept hospitalizations low. We emphasize that

Ottawa's wastewater viral signal rarely reached 0.002 copies/copies PMMov (doing so on 6 days only), so the confidence interval for high wastewater viral signal levels is very wide.

In Fig. 7, we observed that RR for hospitalizations versus time lag appears to be a u-shaped curve during the pre-Omicron period, and an n-shaped curve during the Omicron period. This suggests that the time lag between patients shedding virus and a subsequent increase in hospitalizations was longer during the pre-Omicron period, and shorter during the Omicron period. Possible explanations for the shorter time lag between an increase in viral signal and a subsequent increase in the RR of hospitalization during the Omicron period include the presence of a more transmissible variant capable of immune escape in a population that had largely been protected by public health interventions. This is also discussed in D'Aoust et al. (2022), who note the shorter incubation period with the Omicron BA.1 variant. The 3D plot of the nonlinear lagged association between wastewater viral signals and COVID-19 hospitalizations are also provided (Fig. 8). They illustrate that the lagged association between wastewater viral signal and hospitalizations has evolved over time. In comparing the pre- and post-Omicron time periods, we see that the time lag for hospitalization has been shortened in the Omicron era.

In the supplementary section, we provided further results from our analysis. Figure A.9 shows the estimated time-varying intercept of time $\hat{\alpha} + \hat{f}(t)$ of Model (4). Ideally, $\hat{\alpha} + \hat{f}(t)$ should equal zero which means that the wastewater viral signals and VE fully interpret the Covid-19 hospitalizations. However, the results suggest that there are unexplained features, excluding vaccination and wastewater viral signals. During the pre-Omicron period, $\hat{f}(t)$ continues to increase, and this might be caused by variables not in the model such as properties of variants of concern, for example, those infected by the Delta variant had a

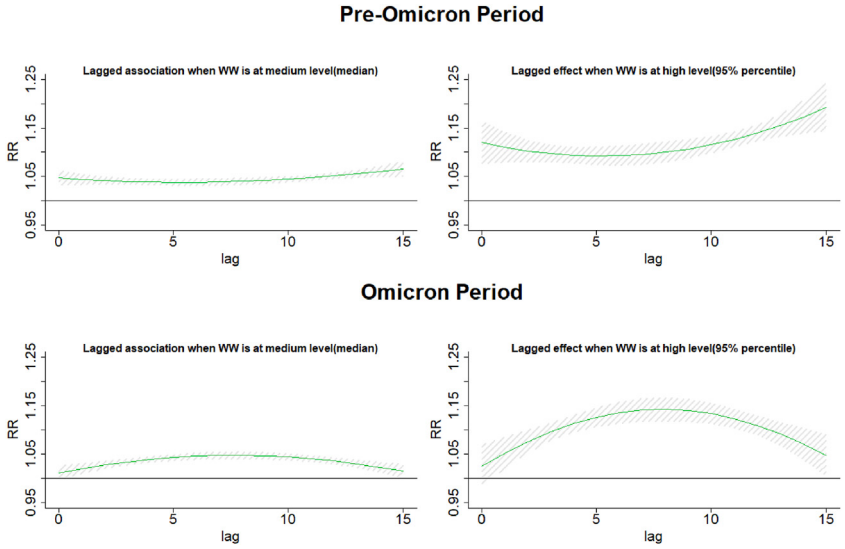

Fig. 7. Relative risk of COVID-19 hospitalizations at specific wastewater viral signals level for pre-Omicron and Omicron period.

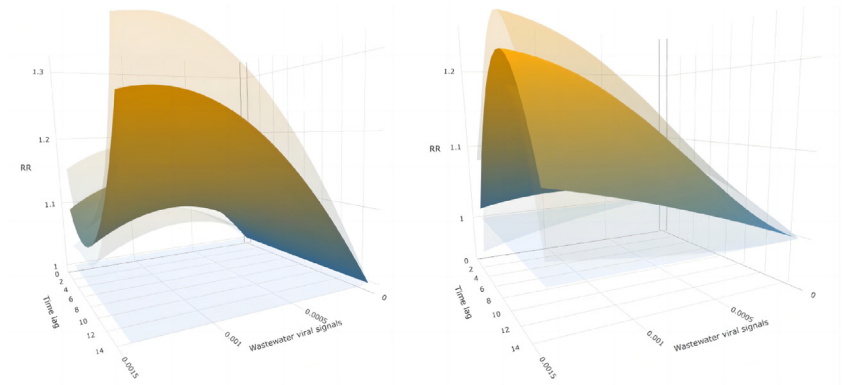

Fig. 8. 3D plot of nonlinear-lagged association between wastewater viral signals and relative risk of COVID-19 hospitalizations for pre-Omicron period(left side), and Omicron period(right side).

higher probability of being hospitalized (Alexandar et al., 2021). Changes to public health policy such as use of masks or closing and re-opening of schools is another feature not accounted for in the model that might affect $\hat{f}(t)$. During the Omicron period, $\hat{\alpha}+\hat{f}(t)$ started at a high level then reduced as Omicron infected people were less likely to be hospitalized (Nyberg et al., 2022). Figure A.10 shows the 3D plot of the nonlinear lagged association between wastewater viral signals and COVID-19 hospitalizations using Model (5). Clearly, the results using Model (4) are more interpretable, although similar features can be observed in Figure A.10 and Fig. 8. We repeated our analysis considering daily hospital admissions as the response variable, instead of the number of patients currently in hospital. The results are shown in Figure A.11 to Figure A.13, and Table A.5. In general, using hospital admissions results in similar conclusions, with less time lag. We decided to use currently in the hospital since the viral signal at day t is also a type of cumulative viral signal in days (not only from that day), with all the infected people including those in the hospital contributing, rather than only newly infected people on the first day of infection. Therefore, we believe the data describing current active hospitalizations as a response variable appropriately matches with measured viral signals in the model.

5. Discussion

5.1. Value of the approach

In this paper, we adapted the rolling correlation method to calculate the optimized Spearman's correlations between wastewater viral signals and COVID-19 hospitalizations. We also provide a simple statistic to investigate how the time-lag between them varies over time. This procedure can also be applied to other data that includes two or more factors that change together, not necessarily at a consistent rate.

In this paper, we studied the relationship between the viral signal of SARS-CoV-2 in Ottawa wastewater versus cases currently in hospital (all hospitalizations including ICU cases). The distributed lag nonlinear model we used accounts for the fact that patients may present to hospital at different times after 'exposure' and that this occurs over a lagged period, i.e., the effect on each individual is different. The distributed lag model fits well with the delayed effect that occurs after exposure to a respiratory pathogen such as SARS-CoV-2, and it is interesting to try to quantify the shape of this lag in the face of changing population immunity and public health interventions. In order to account for the limited data available about individual levels of immune protection, our model also incorporated a method to simulate vaccine effectiveness under different waning assumptions, using estimates from studies of vaccine effectiveness over time.

5.2. Limitations of the data and model

Over the period analyzed here, from March 2020 to November 2022, it may be the case that criteria for admission to hospital changed, with patients more readily admitted to hospital at times when resource use was low. Or, once specific risks were more clearly understood and articulated, those patients who met the criteria of high risk (such as older age groups) were more readily admitted to hospital. There were also changes in health care resource use that may have been driven by population immunity or by variant type, where early in the pandemic we saw a strain on ICU resources, whereas with Omicron and subsequent waves there were fewer admitted to ICU compared to the regular ward.

As mentioned earlier, during the period under analysis, there was a significant change in population immunity, from vaccination campaigns to immunity gained from infection, or both. In addition, during this time period, the province of Ontario went from an initially very high level of protective measures, while transmission was relatively low, to very high levels of transmission under the Omicron era, with progressive lifting of protections to the point where the only remaining protection continues to be masking in health care settings, and masking by personal choice. As we have seen, the scale of these changes in population immunity and non-pharmaceutical interventions have had an impact on the relationship between wastewater signal and hospitalizations. Moving forward, it will be important to carry out analyses that consider the changing levels of population immunity and the implementation of public health interventions, taking into account percentage uptake in new vaccination campaigns. We considered adding seroprevalence data over time from the COVID Immunity Task Force as a covariate, however, this data was available only at the provincial level and is highly correlated with time. Since our time varying intercept, $f(t)$, in our DLNM model explains information that is not included in the model directly, we are able to draw conclusions on wastewater viral signals without seroprevalence data.

5.3. Future investigation

We are currently working on applying the distributed lag model to a larger spatial area, however many important aspects must be considered. Care must be taken when combining data from laboratories that use different methods for collection and analysis. Also, the wastewater treatment plant for the Ottawa region covers a very high percentage of the population (96.1% according to https://613covid.ca/model/#wastewater). Very few public health units in Ontario have this level of coverage, so models will need to be adjusted to account for hospitalizations in the portion of the population not covered by the wastewater

sewershed. This population may be different in ways that affect hospitalization, e.g., they may live in a more rural area, with lower population density and fewer opportunities for transmission.

Referring back to Fig. 8 in Section 4, we can see the evolving landscape that surrounds estimate of future health care resource needs. This landscape changes over time with multiple factors influencing outcomes, including the level of population immunity and the properties of the dominant variant. Wastewater monitoring for SARS-CoV-2 and other pathogens as an indicator for health resource use is improved by including an estimation of changing levels of population immunity. More detailed vaccination data as well as seroprevlence estimates at a fine spatial level, such as from blood donor surveillance, would improve estimation of future health care resource utilization. Moving forward, continued assessment of vaccine protection against hospitalization is an important element to incorporate into health care resource utilization models.

Declaration of competing interest

The authors declare that they have no known competing financial interests or personal relationships that could have appeared to influence the work reported in this paper.

Acknowledgement

The study was supported by the Natural Sciences and Engineering Research Council of Canada (NSERC EIDM). We also thank two anonymous reviewers whose comments helped improve the paper.

Appendix A. Extra figures & tables

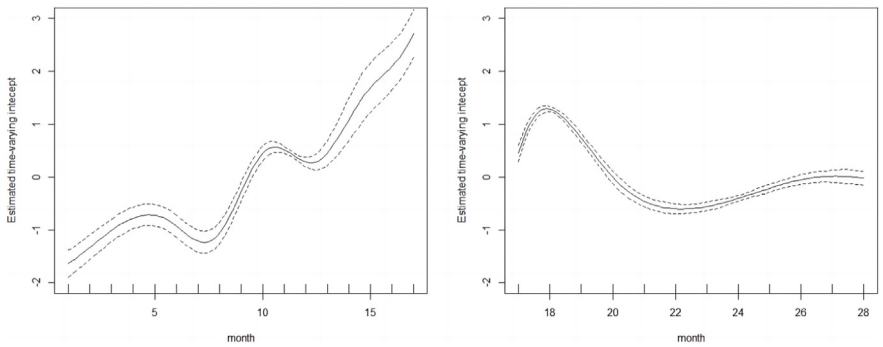

Fig. A.9. $\hat{\alpha}+\hat{f}(t)$ of model (4) for pre-Omicron period (left side), and Omicron period (right side).

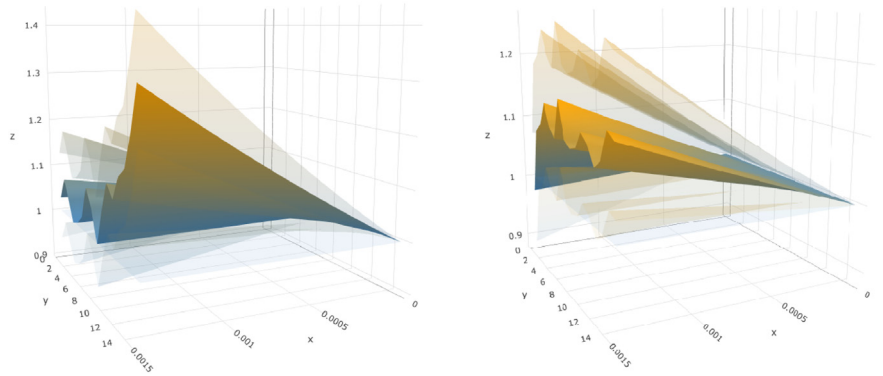

Fig. A.10. 3D plot of nonlinear-lagged association between wastewater viral signals and relative risk of COVID-19 hospitalizations for pre-Omicron period(left side), and Omicron period(right side), using distributed linear lag model.

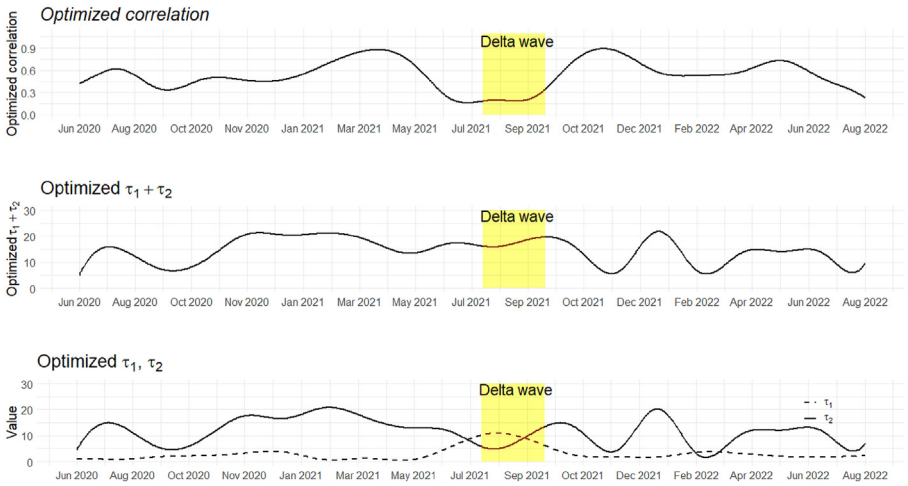

Fig. A.11. The optimized correlation over time (upper plot), the optimized τ_1 + optimized τ_2 over time (middle plot), and optimized τ_1, τ_2 over time. Smoothed using cubic smoothing spline. Using daily hospital admission as response.

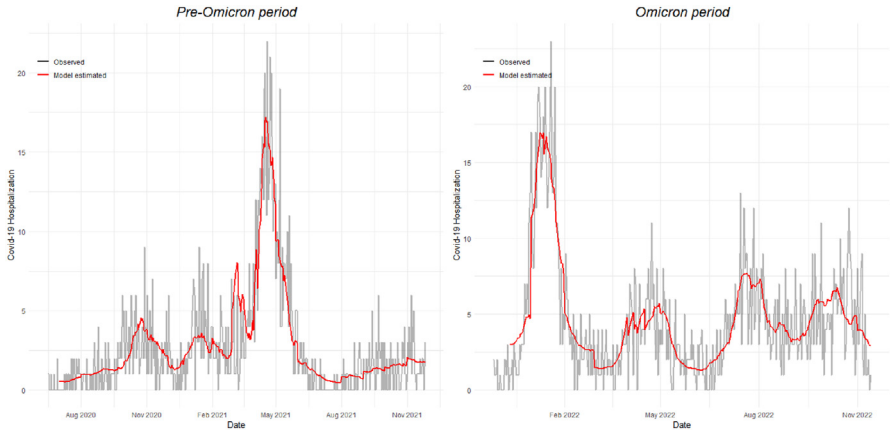

Fig. A.12. Model predicted COVID-19 hospitalizations and observed COVID-19 hospitalizations over time for pre-Omicron and Omicron periods. The model shown is under scenario 3 of the vaccine effectiveness simulation. Using daily hospital admission as response.

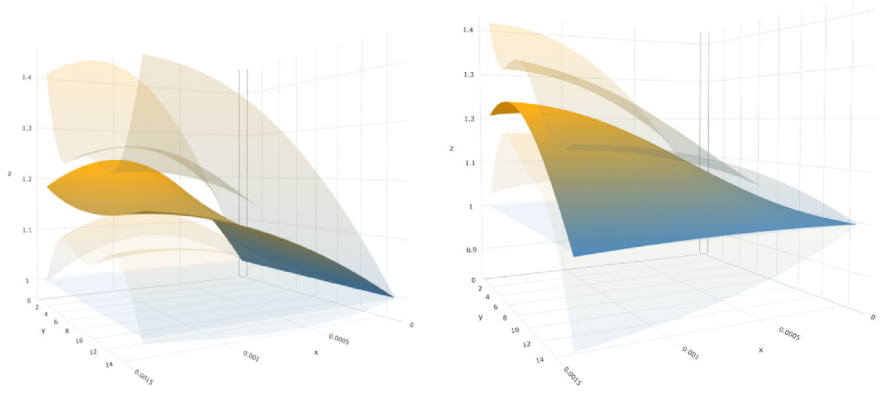

Fig. A.13. 3D plot of nonlinear-lagged association between wastewater viral signals and relative risk of COVID-19 hospitalizations for pre-Omicron period(left side), and Omicron period(right side), using daily hospital admission as response.

Table A.5
Adjusted R^2 and estimated γ of the model under different scenarios using DLNM. The p-value < 0.05 rejects the null hypothesis H_0: $\gamma = 0$. Using admitted number

Scenario	Period	**Adjusted R^2**	AIC	$\hat{\gamma}$ (p-value)
Scenario 1	Pre-Omicron	.721	1815.1	-9.1×10^{-7}(.08)
	Omicron	.645	1496.9	-3.3×10^{-7}(.66)
Scenario 2	Pre-Omicron	.723	1815.2	-1.1×10^{-6}(.09)
	Omicron	.661	1486.7	-2.2×10^{-6}(.00)
Scenario 3	Omicron	.661	1486.9	-2.0×10^{-6}(.00)

References

Alexandar, S., Ravisankar, M., Kumar, R. S., & Jakkan, K. (2021). A comprehensive review on Covid-19 Delta variant. *International Journal of Pharmaceutical Chemistry Research, 5*, 7.

Anand, U., Adelodun, B., Pivato, A., Suresh, S., Indari, O., Jakhmola, S., Jha, H. C., Jha, P. K., Tripathi, V., & Di Maria, F. (2021). A review of the presence of SARS-CoV-2 RNA in wastewater and airborne particulates and its use for virus spreading surveillance. *Environmental Research, 196*, Article 110929.

Andrews, N., Stowe, J., Kirsebom, F., Toffa, S., Rickeard, T., Gallagher, E., Gower, C., Kall, M., Groves, N., O'Connell, A. M., et al. (2022). Covid-19 vaccine effectiveness against the Omicron (B. 1.1. 529) variant. *New England Journal of Medicine, 386*, 1532–1546.

Arabzadeh, R., Grünbacher, D. M., Insam, H., Kreuzinger, N., Markt, R., & Rauch, W. (2021). Data filtering methods for SARS-CoV-2 wastewater surveillance. *Water Science and Technology, 84*, 1324–1339.

Asghar, H., Diop, O. M., Weldegebriel, G., Malik, F., Shetty, S., El Bassioni, L., Akande, A. O., Al Maamoun, E., Zaidi, S., Adeniji, A. J., et al. (2014). Environmental surveillance for polioviruses in the global Polio eradication initiative. *The Journal of Infectious Diseases, 210*, S294–S303.

Dai, X., Champredon, D., Fazil, A., Mangat, C. S., Peterson, S. W., Mejia, E. M., Lu, X., & Chekouo, T. (2022). Statistical framework to support the epidemiological interpretation of SARS-CoV-2 concentration in municipal wastewater. *Scientific Reports, 12*, 1–10.

D'Aoust, P. M., Graber, T. E., Mercier, E., Montpetit, D., Alexandrov, I., Neault, N., Baig, A. T., Mayne, J., Zhang, X., Alain, T., et al. (2021a). Catching a resurgence: Increase in SARS-CoV-2 viral RNA identified in wastewater 48 h before COVID-19 clinical tests and 96 h before hospitalizations. *Science of The Total Environment, 770*, Article 145319.

D'Aoust, P. M., Mercier, E., Montpetit, D., Jia, J. J., Alexandrov, I., Neault, N., Baig, A. T., Mayne, J., Zhang, X., Alain, T., et al. (2021b). Quantitative analysis of SARS-CoV-2 RNA from wastewater solids in communities with low COVID-19 incidence and prevalence. *Water Research, 188*, Article 116560.

D'Aoust, P. M., Tian, X., Towhid, S. T., Xiao, A., Mercier, E., Hegazy, N., Jia, J. J., Wan, S., Kabir, M. P., Fang, W., et al. (2022). Wastewater to clinical case (WC) ratio of COVID-19 identifies insufficient clinical testing, onset of new variants of concern and population immunity in urban communities. *Science of The Total Environment, 853*, Article 158547.

Eilers, P. H., & Marx, B. D. (1996). Flexible smoothing with B-splines and penalties. *Statistical Science, 11*, 89–121.

Entezari, A., & Mayvaneh, F. (2019). Applying the distributed lag non-linear model (DLNM) in epidemiology: Temperature and mortality in Mashhad. *Iranian Journal of Public Health, 48*, 2108.

Feng, L., Zhang, W., & Li, X. (2018). Monitoring of regional drug abuse through wastewater-based epidemiology—a critical review. *Science China Earth Sciences, 61*, 239–255.

Ferdinands, J. M., Rao, S., Dixon, B. E., Mitchell, P. K., DeSilva, M. B., Irving, S. A., Lewis, N., Natarajan, K., Stenehjem, E., Grannis, S. J., et al. (2022). *Waning of vaccine effectiveness against moderate and severe covid-19 among adults in the US from the VISION network: Test negative, case-control study* (p. 379). bmj.

Galani, A., Aalizadeh, R., Kostakis, M., Markou, A., Alygizakis, N., Lytras, T., Adamopoulos, P. G., Peccia, J., Thompson, D. C., Kontou, A., et al. (2022). SARS-CoV-2 wastewater surveillance data can predict hospitalizations and ICU admissions. *Science of The Total Environment, 804*, Article 150151.

Gasparrini, A., Armstrong, B., & Kenward, M. G. (2010). Distributed lag non-linear models. *Statistics in Medicine, 29*, 2224–2234.

Guo, W., Yi, L., Wang, P., Wang, B., & Li, M. (2021). The effect of air temperature on hospital admission of adults with community acquired pneumonia in Baotou, China. *Scientific Reports, 11*, 1–7.

Hegazy, N., Cowan, A., D'Aoust, P. M., Mercier, E., Towhid, S. T., Jia, J. J., Wan, S., Zhang, Z., Kabir, M. P., Fang, W., et al. (2022). *Understanding the dynamic relation between wastewater SARS-CoV-2 signal and clinical metrics throughout the pandemic*. medRxiv.

Judge, G. G. (1982). *Introduction to the theory and practice of econometrics*.

Kaplan, E. H., Wang, D., Wang, M., Malik, A. A., Zulli, A., & Peccia, J. (2021). Aligning SARS-CoV-2 indicators via an epidemic model: Application to hospital admissions and RNA detection in sewage sludge. *Health Care Management Science, 24*, 320–329.

Larsen, D. A., & Wigginton, K. R. (2020). Tracking COVID-19 with wastewater. *Nature Biotechnology, 38*, 1151–1153.

Larson, P. S., Espira, L., Glenn, B. E., Larson, M. C., Crowe, C. S., Jang, S., & O'Neill, M. S. (2022). Long-term PM2. 5 exposure is associated with symptoms of acute respiratory infections among children under five years of age in Kenya, 2014. *International Journal of Environmental Research and Public Health, 19*, 2525.

Medema, G., Heijnen, L., Elsinga, G., Italiaander, R., & Brouwer, A. (2020). Presence of SARS-Coronavirus-2 RNA in sewage and correlation with reported COVID-19 prevalence in the early stage of the epidemic in The Netherlands. *Environmental Science and Technology Letters, 7*, 511–516.

Nyberg, T., Ferguson, N. M., Nash, S. G., Webster, H. H., Flaxman, S., Andrews, N., Hinsley, W., Bernal, J. L., Kall, M., Bhatt, S., et al. (2022). Comparative analysis of the risks of hospitalisation and death associated with SARS-CoV-2 omicron (B. 1.1. 529) and delta (B. 1.617. 2) variants in england: A cohort study. *The Lancet, 399*, 1303–1312.

Peccia, J., Zulli, A., Brackney, D. E., Grubaugh, N. D., Kaplan, E. H., Casanovas-Massana, A., Ko, A. I., Malik, A. A., Wang, D., Wang, M., et al. (2020). Measurement of SARS-CoV-2 RNA in wastewater tracks community infection dynamics. *Nature Biotechnology, 38*, 1164–1167.

Pedder, H., Kapwata, T., Howard, G., Naidoo, R. N., Kunene, Z., Morris, R. W., Mathee, A., & Wright, C. Y. (2021). Lagged association between climate variables and hospital admissions for pneumonia in South Africa. *International Journal of Environmental Research and Public Health, 18*, 6191.

Pope, C. A., III, & Schwartz, J. (1996). Time series for the analysis of pulmonary health data. *American Journal of Respiratory and Critical Care Medicine, 154*, S229.

Randazzo, W., Truchado, P., Cuevas-Ferrando, E., Simón, P., Allende, A., & Sánchez, G. (2020). SARS-CoV-2 RNA in wastewater anticipated COVID-19 occurrence in a low prevalence area. *Water Research, 181*, Article 115942.

Rousis, N. I., Gracia-Lor, E., Zuccato, E., Bade, R., Baz-Lomba, J. A., Castrignanò, E., Causanilles, A., Covaci, A., de Voogt, P., Hernàndez, F., et al. (2017). Wastewater-based epidemiology to assess pan-European pesticide exposure. *Water Research, 121*, 270–279.

Schoen, M. E., Wolfe, M. K., Li, L., Duong, D., White, B. J., Hughes, B., & Boehm, A. B. (2022). SARS-CoV-2 RNA wastewater settled solids surveillance frequency and impact on predicted COVID-19 incidence using a distributed lag model. *ACS ES&T Water, 2*(11), 2167–2174.

Ssentongo, P., Ssentongo, A. E., Voleti, N., Groff, D., Sun, A., Ba, D. M., Nunez, J., Parent, L. J., Chinchilli, V. M., & Paules, C. I. (2022). SARS-CoV-2 vaccine effectiveness against infection, symptomatic and severe COVID-19: A systematic review and meta-analysis. *BMC Infectious Diseases, 22*, 1–12.

Thompson, M. G. (2022). *Effectiveness of a third dose of mRNA vaccines against COVID-19—associated emergency department and urgent care encounters and hospitalizations among adults during periods of Delta and Omicron variant predominance—VISION Network, 10 States, August 2021–January 2022. MMWR. Morbidity and Mortality Weekly Report 71*.

Xie, Y., Challis, J. K., Oloye, F. F., Asadi, M., Cantin, J., Brinkmann, M., McPhedran, K. N., Hogan, N., Sadowski, M., Jones, P. D., et al. (2022). *RNA in municipal wastewater reveals magnitudes of COVID-19 outbreaks across four waves driven by SARS-CoV-2 variants of concern*. ACS ES&T Water.

Zuccato, E., Chiabrando, C., Castiglioni, S., Bagnati, R., & Fanelli, R. (2008). Estimating community drug abuse by wastewater analysis. *Environmental Health Perspectives, 116*, 1027–1032.

Zuccato, E., Chiabrando, C., Castiglioni, S., Calamari, D., Bagnati, R., Schiarea, S., & Fanelli, R. (2005). Cocaine in surface waters: A new evidence-based tool to monitor community drug abuse. *Environmental Health, 4*, 1–7.

Zulli, A., Pan, A., Bart, S. M., Crawford, F. W., Kaplan, E. H., Cartter, M., Ko, A. I., Sanchez, M., Brown, C., Cozens, D., et al. (2022). Predicting daily COVID-19 case rates from SARS-CoV-2 RNA concentrations across a diversity of wastewater catchments. *FEMS microbes, 2*.